

Structural Elucidation of  $\beta_1$ - and  $\beta_2$ -Transferrin Using Microprobe-Capture In-Emitter Elution  
and High-Resolution Mass Spectrometry

Ruben Yiqi Luo<sup>1,2</sup>, Christopher Pfaffroth<sup>2</sup>, Samuel Yang<sup>1</sup>, Kevin Hoang<sup>2</sup>, Priscilla S.-W.

Yeung<sup>1,2</sup>, James L. Zehnder<sup>1,2</sup>, Run-Zhang Shi<sup>1,2</sup>

<sup>1</sup>Department of Pathology, Stanford University, Stanford, CA, USA

<sup>2</sup>Clinical Laboratories, Stanford Health Care, Palo Alto, CA, USA

Running Title: Structural Elucidation of  $\beta_1$ - and  $\beta_2$ -Tf Using MPIE and HR-MS

Corresponding Author: Ruben Yiqi Luo

Address: 3375 Hillview Ave, Palo Alto, CA 94304

Tel: 650-724-1318

Email: [rubenluo@stanford.edu](mailto:rubenluo@stanford.edu)

Key Words:  $\beta_1$ -Transferrin,  $\beta_2$ -Transferrin, MPIE-ESI-MS, N-Glycan

1 **Abstract**

2

3 Background: Cerebrospinal fluid (CSF) leak is typically diagnosed by detecting a protein marker  
4  $\beta_2$ -transferrin ( $\beta_2$ -Tf) in secretion samples.  $\beta_2$ -Tf and  $\beta_1$ -transferrin ( $\beta_1$ -Tf) are glycoforms of  
5 human transferrin (Tf). A novel affinity capture technique for sample preparation, called  
6 microprobe-capture in-emitter elution (MPIE), was incorporated with high-resolution mass  
7 spectrometry (HR-MS) to analyze the Tf glycoforms and elucidate the structures of  $\beta_1$ -Tf and  $\beta_2$ -  
8 Tf.

9 Methods: To implement MPIE, an analyte is first captured on the surface of a microprobe, and  
10 subsequently eluted from the microprobe inside an electrospray emitter. The capture process is  
11 monitored in real-time via next-generation biolayer interferometry (BLI). When electrospray is  
12 established from the emitter to a mass spectrometer, the analyte is immediately ionized via  
13 electrospray ionization (ESI) for HR-MS analysis. Serum, CSF, and secretion samples were  
14 analyzed using MPIE-ESI-MS.

15 Results: Based on the MPIE-ESI-MS results, the structures of  $\beta_1$ -Tf and  $\beta_2$ -Tf were solved. As Tf  
16 glycoforms,  $\beta_1$ -Tf and  $\beta_2$ -Tf share the amino acid sequence but have varying N-glycans.  $\beta_1$ -Tf,  
17 the major serum-type Tf, has two G2S2 N-glycans on Asn413 and Asn611.  $\beta_2$ -Tf, the major  
18 brain-type Tf, has an M5 N-glycan on Asn413 and a G0FB N-glycan on Asn611.

19 Conclusions: The structures of  $\beta_1$ -Tf and  $\beta_2$ -Tf were successfully elucidated by MPIE-ESI-MS  
20 analysis. The resolving power of the novel MPIE-ESI-MS method was demonstrated in this  
21 study. On the other hand, knowing the N-glycan structures on  $\beta_2$ -Tf allows for the design of  
22 other novel test methods for  $\beta_2$ -Tf in the future.

23

## 24 **Introduction**

25  
26 Cerebrospinal fluid (CSF) leak can occur as a result of laceration, blunt trauma, or surgery. It  
27 may lead to potentially life-threatening meningitis if left untreated (1,2). Because  $\beta_2$ -transferrin  
28 ( $\beta_2$ -Tf), a proteoform of human transferrin (Tf), is mainly present in CSF and barely detectable in  
29 other body fluids (3,4), CSF leak can be diagnosed by detecting  $\beta_2$ -Tf in any body fluid – most  
30 commonly in rhinorrhea or otorrhea secretion samples. The clinical utility and diagnostic value  
31 of  $\beta_2$ -Tf in CSF leak have been demonstrated (5,6).  $\beta_2$ -Tf, together with the typical Tf  
32 proteoform in serum  $\beta_1$ -transferrin ( $\beta_1$ -Tf), were named after their electrophoretic mobility in gel  
33 electrophoresis (7). However, the structures of  $\beta_1$ -Tf and  $\beta_2$ -Tf have not been elucidated.

34  
35 There has been extensive basic research on human Tf since it is a high-abundance protein in  
36 human blood with a major role in iron metabolism. The amino acid sequence of Tf precursor was  
37 determined through protein cleavage and cDNA characterization, showing a full sequence of 698  
38 amino acids; after the removal of an N-terminal signal peptide, the mature form of Tf contains  
39 679 amino acids, 19 intramolecular disulfide bonds formed between cysteine residues, and two  
40 N-glycans attached to the amino groups of the side chains of Asn419 and Asn611 (Asn432 and  
41 Asn630 of Tf precursor) (8–11). Tf proteoforms typically vary by the N-glycan structures (11–  
42 13), and the Tf proteoforms of interest so far are Tf glycoforms, including  $\beta_1$ -Tf and  $\beta_2$ -Tf (7).

43  
44 Although it is known that  $\beta_2$ -Tf has desialylated N-glycans while  $\beta_1$ -Tf has fully sialylated N-  
45 glycans (3,14,15), the structures of  $\beta_1$ -Tf and  $\beta_2$ -Tf have not been clarified. On the other hand,  
46 the N-glycans on Tf glycoforms in serum and in CSF were characterized using gel

47 electrophoresis, liquid chromatography, and enzymatic digestion-based mass spectrometry (MS)  
48 by neurobiologists (13,16–19). It was reported that a group of Tf glycoforms were present in  
49 serum, namely serum-type Tf or sTf, among which a specific Tf glycoform (major serum-type  
50 Tf) predominated (12,13); the serum-type Tf also existed in CSF, and the major serum-type Tf  
51 used to be named Tf-2 in CSF (18); an additional group of Tf glycoforms were present in CSF,  
52 namely brain-type Tf or Tf-1 in CSF, among which a specific Tf glycoform (major brain-type  
53 Tf) was more abundant than the rest (15,20). The brain-type Tf was at least partly synthesized in  
54 the CSF-producing tissue choroid plexus rather than being produced by glycosidase digestion of  
55 serum-type Tf (16,20). It was found that the N-glycans on the major serum-type Tf consisted of  
56 bi-antennary oligosaccharide chains with sialylated terminals, and those on the brain-type Tf are  
57 desialylated, or more specifically, unsialylated (asialotransferrin) (15,16,18,20). It was  
58 hypothesized that the major brain-type Tf was  $\beta_2$ -Tf (21), but this hypothesis has not been  
59 proved.

60  
61 In clinical cases where CSF leak is suspected, secretion samples can be collected from patients  
62 and sent to clinical laboratories to test for the presence of  $\beta_2$ -Tf. The conventional method to test  
63  $\beta_2$ -Tf as well as  $\beta_1$ -Tf is agarose gel immunofixation electrophoresis (IFE) (2–4). Although it is  
64 widely used in clinical laboratories, it does not provide structural information of the analytes.  
65 Thus, the structures of  $\beta_1$ -Tf and  $\beta_2$ -Tf, particularly the N-glycan structures on these Tf  
66 glycoforms, remained an unanswered question with this method.

67  
68 As an emerging technology in clinical diagnostics, high-resolution mass spectrometry (HR-MS),  
69 particularly top-down HR-MS, can be used to analyze a protein target in its intact state and

70 elucidate the post-translational modifications and amino acid variations in its proteoforms (22–  
71 24). While HR-MS is an ideal tool to analyze the Tf glycoforms, the quality of data acquired  
72 during HR-MS analysis depends on sample preparation (25,26). In this article, a novel affinity  
73 capture technique for sample preparation, called microprobe-capture in-emitter elution (MPIE),  
74 was incorporated with HR-MS to study the Tf glycoforms (27). MPIE can directly couple a  
75 label-free optical sensing technology with MS. The label-free optical sensing technology is next-  
76 generation biolayer interferometry (BLI, also named as thin-layer interferometry, TFI), which  
77 senses optical thickness changes on the sensing surface of a microprobe caused by biomolecular  
78 interactions, achieving real-time measurement without employing a reporter molecule (enzyme,  
79 fluorophore, etc.) (28,29). To implement MPIE, an analyte is first captured on the surface of a  
80 microprobe, and subsequently eluted from the microprobe inside an electrospray emitter. The  
81 capture process is monitored in real-time via BLI. When electrospray is established from the  
82 emitter to a mass spectrometer, the analyte is immediately ionized via electrospray ionization  
83 (ESI) for HR-MS analysis. By this means, BLI and HR-MS are directly coupled in the form of  
84 MPIE-ESI-MS, which is readily deployed to analyze the Tf glycoforms and elucidate the  
85 structures of  $\beta_1$ -Tf and  $\beta_2$ -Tf. The study can pave a way for the development of novel clinical  
86 assays for  $\beta_2$ -Tf.

87

## 88 **Materials and Methods**

89

### 90 Materials and Specimens

91

92 LC-MS grade water, acetonitrile, formic acid, and 0.2  $\mu$ m PVDF syringe filters were purchased  
93 from Thermo Fisher Scientific (Waltham, MA). Tf standard (purified sTf) was purchased from  
94 Sigma-Aldrich (St. Louis, MI). A mouse monoclonal anti-transferrin IgG antibody (anti-Tf Ab)  
95 was obtained from Sinobiological (Wayne, PA), and biotinylated using an EZ-Link HPDP-Biotin  
96 reagent kit (Waltham, MA). Remnant CSF and serum samples from patients, and secretion  
97 samples from patients suspected of CSF leak were obtained from Stanford Health Care and  
98 Stanford Children's Health, following approved institutional review board protocols for the use  
99 of remnant patient specimens.

100

#### 101 Sample Preparation

102

103 The biotinylated anti-Tf Ab was diluted in phosphate-buffered saline at pH 7.4 with 0.02%  
104 Tween 20 and 0.2% BSA (PBST-B) to 10  $\mu$ g/ml for use. A pooled CSF sample was made by  
105 mixing 9 CSF samples from patients to explore the analytical sensitivity of MPIE-ESI-MS for  
106  $\beta_2$ -Tf in CSF. The pooled CSF sample was mixed with water to make a dilution series. All CSF  
107 samples were 1:1 diluted in phosphate-buffered saline at pH 7.4 with 0.02% Tween 20 (PBST)  
108 and all serum samples were 1:19 diluted in PBST-B. Secretion samples from patients were first  
109 mixed with an equal amount of water and filtered using a 0.2  $\mu$ m PVDF syringe filter, and then  
110 1:1 diluted in PBST.

111

112 To study the gel electrophoresis-separated Tf glycoforms, gel electrophoresis of CSF samples  
113 was carried out using a Hydragel 6  $\beta_2$  Transferrin kit (Sebia, Lisses, France) following the  
114 manufacturer's protocol. In brief, a CSF sample was first 1:1 mixed with an iron-saturating

115 solution, and then 10  $\mu$ l of the sample was loaded to each of the 6 wells on an agarose gel. Gel  
116 electrophoresis was implemented in a Hydrasys 2 instrument (Sebia, Lisses, France), and the  
117 agarose gel was removed from the instrument after the gel electrophoresis was completed,  
118 without running the immunofixation steps. The agarose gel was placed on a paper template  
119 marked with the  $\beta_1$ -Tf and  $\beta_2$ -Tf band regions, and the gel stripes of the band regions were cut  
120 out using a scalpel. Each gel stripe was placed in a 1.5 ml sample tube, 200  $\mu$ l PBST was added,  
121 and the sample was rocked for 2 hr at room temperature to extract the analyte from the gel stripe.  
122 After extraction, the supernatant was filtered using a 0.2  $\mu$ m PVDF syringe filter.

123

#### 124 MPIE-ESI-MS Instrumentation and Experiment

125

126 An MPIE-ESI-MS experiment consists of two parts: BLI-based affinity capture and in-emitter  
127 elution ESI-MS, with the details including instrumentation described elsewhere (27). The BLI-  
128 based affinity capture was implemented in a Gator Plus analyzer (Gator Bio, Palo Alto, CA): a  
129 BLI microprobe pre-coated with streptavidin was first dipped into the biotinylated anti-Tf Ab  
130 solution for 10 min to load the anti-Tf Ab, then dipped into a sample for 10 min to capture Tf  
131 molecules, and rinsed in PBST for 1 min to remove non-specifically bound molecules. The in-  
132 emitter elution ESI-MS was implemented in an EMASS-II ESI ion source which coupled an  
133 ECE-001 capillary electrophoresis instrument (CMP Scientific, Brooklyn, NY) with an Orbitrap  
134 Q-Exactive Plus mass spectrometer (Thermo Scientific, San Jose, CA): an electrospray emitter  
135 with a regular open end and a tapered open end (tip orifice diameter 20-30  $\mu$ m) was filled with a  
136 sheath liquid (10 mM ammonium formate in water); after affinity capture, the microprobe was  
137 rinsed in the sheath liquid for 10 s, inserted into the emitter through the regular open end, and

138 settled in the tapered end by gravity; the emitter was mounted to the ESI ion source, and a  
139 capillary was inserted into the emitter through the regular open end and positioned right behind  
140 the microprobe to deliver an elution liquid (80% acetonitrile and 2% formic acid in water); once  
141 electrospray was established by applying a positive voltage to the sheath liquid in the emitter,  
142 HR-MS data acquisition was initiated, and injection of the elution liquid was started  
143 subsequently. The emitter was placed ~2 mm away from the mass spectrometer inlet with the  
144 electrospray voltage set at 2.2 kV. The injection of the elution liquid was driven by 5 psi  
145 pneumatic pressure. The following MS parameters were used: ion-transfer capillary temperature  
146 350°C, S-lens RF level 50, and number of microscans 10. Primary mass spectra were acquired in  
147 positive polarity at resolution 17.5K.

148

#### 149 Data Analysis

150

151 In HR-MS analysis of proteins, it is necessary to deconvolute raw MS data to merge the multiple  
152 charge states and isotopic peaks of an analyte to obtain its accurate molecular mass. The acquired  
153 data in each MPIE-ESI-MS experiment was viewed as a time trace of MS responses, and the  
154 elution time window of an analyte was identified by checking the molecular ions of the analyte at  
155 each time point. The data in the elution time window were selected for deconvolution using  
156 Biopharma Finder 4.1 (Thermo Fisher Scientific, San Jose, CA) with the ReSpect algorithm. MS  
157 peaks of analytes were displayed in deconvoluted mass spectra at uncharged state showing  
158 average molecular masses.

159

#### 160 **Results**



161  
162 The performance of MPIE-ESI-MS for Tf analysis was demonstrated and reported elsewhere  
163 (27). MPIE-ESI-MS had a limit of detection for the Tf standard at 0.063  $\mu\text{g/ml}$ , which was  
164 translated to no more than 7 fmol Tf molecules captured on a microprobe (27). The high  
165 analytical sensitivity and specificity provided by affinity capture made MPIE-ESI-MS an ideal  
166 method to study the Tf molecules in serum, CSF, and secretion samples. The results of a set of  
167 samples are shown in Figure 1. The deconvoluted mass spectrum of the serum sample showed a  
168 group of MS peaks around 79554 Da; they are mainly serum-type Tf glycoforms and the  
169 predominant MS peak at 79554 Da should be the major serum-type Tf (N-glycan structures  
170 shown in Figure 1, see details in Discussion). The deconvoluted mass spectrum of the CSF  
171 sample showed the major serum-type Tf and a group of MS peaks around 78008 Da; they are  
172 mainly brain-type Tf glycoforms and the most abundant MS peak at 78008 Da should be the  
173 major brain-type Tf (N-glycan structures shown in Figure 1, see details in Discussion). The  
174 deconvoluted mass spectrum of the secretion sample showed both serum-type Tf and brain-type  
175 Tf glycoforms, meaning that CSF was present in the sample. This finding was consistent with the  
176 fact that the secretion sample was obtained from a patient diagnosed of CSF leak. In addition, the  
177 BLI sensorgram (a time trace of label-free optical sensing responses) of each affinity capture  
178 process (capture of Tf by anti-Tf Ab on a microprobe) is shown in Figure S1, allowing for real-  
179 time monitoring of the capture process.

180  
181 To elucidate the structures of the Tf glycoforms  $\beta_1$ -Tf and  $\beta_2$ -Tf, after gel electrophoresis of CSF  
182 samples, the extracts from the gel stripes of the  $\beta_1$ -Tf and  $\beta_2$ -Tf band regions were analyzed  
183 using MPIE-ESI-MS. The results of a set of samples are shown in Figure 2. The deconvoluted

184 mass spectra showed the MS peak of only the major serum-type Tf in the extract from the  $\beta_1$ -Tf  
185 band region and the MS peak of only the major brain-type Tf in the extract from the  $\beta_2$ -Tf band  
186 region. The measured accurate molecular masses were consistent with the experiments in Figure  
187 1 and matched the theoretical molecular masses of the major serum-type Tf and major brain-type  
188 Tf (N-glycan structures shown in Figure 2, see details in Discussion). This observation  
189 confirmed that  $\beta_1$ -Tf and  $\beta_2$ -Tf were actually the major serum-type Tf and major brain-type Tf,  
190 respectively. In addition, the gel area between the  $\beta_1$ -Tf and  $\beta_2$ -Tf band regions was also  
191 analyzed and minor Tf glycoforms in serum and CSF were found, which could be due to the low  
192 abundance of the minor Tf glycoforms and limited analyte quantities in a gel stripe.

193  
194 A set of 12 secretion samples from patients suspected of CSF leak were analyzed using the  
195 MPIE-ESI-MS method, among which 5 samples were positive for  $\beta_2$ -Tf and the rest were  
196 negative as measured by IFE test and clinical manifestations. As shown in Table 1, the MS peak  
197 at 78008 Da was observed in the MPIE-ESI-MS results of the 5 positive samples but not found  
198 in those of the 7 negative samples, which further verified that  $\beta_2$ -Tf was indeed the major brain-  
199 type Tf. In addition, the analytical sensitivity of the MPIE-ESI-MS method for CSF and  
200 secretion samples was explored. A pooled CSF sample was mixed with water at 1:1, 1:4, 1:9, and  
201 1:19 ratios to prepare a dilution series for analysis. Table S1 summarizes the results, listing the  
202 MS peak intensities of  $\beta_1$ -Tf and  $\beta_2$ -Tf in the deconvoluted mass spectra (the entire time window  
203 of Tf elution selected for deconvolution). The peak intensities decreased with the pooled CSF  
204 sample dilution, and it was demonstrated that the MPIE-ESI-MS method was able to detect  $\beta_2$ -Tf  
205 in at least 10-fold diluted CSF (1:9 pooled CSF : water mixture).

206

207 **Discussion**

208

209 The amino acid sequence of Tf was previously reported (8,9) and the primary structure of a  
210 mature Tf molecule is illustrated in Figure 3A. As Tf glycoforms,  $\beta_1$ -Tf and  $\beta_2$ -Tf share the  
211 amino acid backbone but have varying N-glycans. The N-glycans on proteins typically include  
212 bi-, tri-, or tetra-antennary oligosaccharide chains, resulted from sequential action of  
213 glycosyltransferases (30,31). An N-glycan can be named according to its sugar composition and  
214 branching structure using a few nomenclature systems (traditional nomenclature used in this  
215 article) (32). With designated N-glycan types, the accurate molecular mass of a Tf glycoform can  
216 be calculated, and the correctness of the N-glycan types can be confirmed by comparing the  
217 theoretical molecular mass of the Tf glycoform to the measured accurate molecular mass.

218

219 Regarding the N-glycans on Tf, the previous enzymatic digestion-based MS analysis of the Tf  
220 glycoforms in CSF revealed explicitly that the most abundant N-glycan type was G2S2 (17,19).  
221 By measuring the trypsin-digested peptides encompassing the glycosylation sites, G2S2 was  
222 found consisting of roughly 65% of all N-glycans on Asn413 and 73% of all N-glycans on  
223 Asn611 (17). Thus, the Tf glycoform with two G2S2 N-glycans on Asn413 and Asn611 is the  
224 major serum-type Tf because (1) it is the most abundant Tf glycoform in serum and CSF, (2) it is  
225 fully sialylated (N-acetylneuraminic acid as the sialic acid), and (3) its theoretical molecular  
226 mass 79554.71 Da exactly matches the measured molecular mass of the major serum-type Tf  
227 (Figure 3B). As the second most abundant Tf glycoform and the most abundant unsialylated Tf  
228 glycoform in CSF, the major brain-type Tf should be associated with N-glycan types M5 and  
229 G0FB (Figure 3B), which were found as the most abundant unsialylated N-glycans (19).

230 Particularly, M5 was found consisting of roughly 20% of all N-glycans on Asn413 and G0FB  
231 was found consisting of 26% of all N-glycans on Asn611 (17). Thus, the major brain-type Tf has  
232 an M5 N-glycan on Asn413 and a G0FB N-glycan on Asn611. Its theoretical molecular mass  
233 78008.35 Da exactly matches the measured molecular mass of the major brain-type Tf. The  
234 glycosylation sites of the M5 and G0FB N-glycans were confirmed with another study of  
235 trypsin-digested glycopeptides from Tf glycoforms in CSF (18). In addition, the presence of a  
236 bisecting N-acetylglucosamine (GlcNAc) in the G0FB N-glycan was proved by the previously  
237 reported lectin-binding experiments (16), supporting that G0FB is the more favorable N-glycan  
238 type on Asn611 than the other isomeric N-glycan type without a bisecting GlcNAc (19). In  
239 addition, the MPIE-ESI-MS analysis of the extracts from the gel bands proved that  $\beta_1$ -Tf and the  
240 major serum-type Tf were identical, so were  $\beta_2$ -Tf and the major brain-type Tf.

241  
242 Besides the two major Tf glycoforms in CSF ( $\beta_1$ -Tf and  $\beta_2$ -Tf), it is known that other minor Tf  
243 glycoforms may also exist in CSF, blood, and other body fluids (4,33). As illustrated in the  
244 previous literature, there are a variety of unsialylated N-glycans on Tf molecules, and the  
245 sialylated N-glycan G2S2 also has diversity such as the more branched form G3S3 (13,17,34).  
246 Thus, a number of fully sialylated, partially sialylated, and unsialylated Tf glycoforms can be  
247 formed by the various combinations of the two N-glycans on a Tf molecule. In gel  
248 electrophoresis, sialic acids bring negative charges to a Tf molecule under neutral or alkaline pH  
249 conditions, influencing its electrophoretic mobility. As such, Tf glycoforms migrate in the order  
250 of fully sialylated, disialylated, and unsialylated Tf glycoforms, with regard to the number of  
251 sialic acids on the N-glycans. Thus, the minor Tf glycoforms can migrate within or between the  
252  $\beta_1$ -Tf and  $\beta_2$ -Tf band regions. For instance, the product insert of the Hydrigel 6  $\beta_2$  Transferrin kit

253 states that a band of disialylated Tf glycoforms (disialotransferrin) may exist above the  $\beta_2$ -Tf  
254 band (35). On the other hand, the unsialylated Tf glycoforms besides  $\beta_2$ -Tf can migrate within  
255 the  $\beta_2$ -Tf band region and interfere with the  $\beta_2$ -Tf detection. The product insert suggests that the  
256 ratio of unsialylated to disialylated bands can be used to confirm the presence of  $\beta_2$ -Tf. The  
257 reason of this practice can be explained as follows: when CSF is present in a sample, the  
258 abundance of the major unsialylated Tf glycoform  $\beta_2$ -Tf significantly exceeds the minor  
259 unsialylated and disialylated Tf glycoforms, resulting in a high ratio of the  $\beta_2$ -Tf band to the  
260 disialotransferrin band. This practice in IFE is derived from the lack of molecular structure  
261 information in gel electrophoresis. However, when MS is employed, such as in the use of MPIE-  
262 ESI-MS, it is unnecessary to compare unsialylated and disialylated Tf glycoforms because  $\beta_2$ -Tf  
263 can be specifically detected by its accurate molecular mass, definitively differentiating it from  
264 the other Tf glycoforms with different molecular masses.

265  
266 The demonstration of MPIE-ESI-MS in detection of  $\beta_2$ -Tf paved a way to establish a MS-based  
267 clinical assay for  $\beta_2$ -Tf. However, more factors need to be taken into consideration for this  
268 purpose. When implementing the accurate molecular mass-based detection of  $\beta_2$ -Tf, Tf variants  
269 resulted from genetic polymorphism should be taken into consideration (11,36–39). In theory,  
270 the amino acid mutations in Tf variants affect the molecular masses of  $\beta_1$ -Tf and  $\beta_2$ -Tf, but they  
271 should not change the molecular mass difference between the two Tf glycoforms (1546 Da),  
272 provided the two glycosylation sites are not modified. This hypothesis is supported by the MPIE-  
273 ESI-MS results of a few Tf variant-containing CSF samples, as shown in Figure S2, but it needs  
274 to be proved with a larger number of Tf variant samples. In addition, the glycoforms in serum-  
275 type Tf can vary under specific pathophysiological conditions and  $\beta_1$ -Tf might not be found in

276 those samples due to aberrant glycosylation (12,34). In such cases the detection and  
277 identification of  $\beta_2$ -Tf can be impacted. These topics are beyond the scope of this article and can  
278 be investigated in the future when a MS-based clinical assay for  $\beta_2$ -Tf is being developed.

279

## 280 **Conclusions**

281

282 The structures of  $\beta_1$ -Tf and  $\beta_2$ -Tf were successfully elucidated by MPIE-ESI-MS analysis. The  
283 resolving power of the novel MPIE-ESI-MS method was demonstrated in this study. As an  
284 innovative affinity capture technique, MPIE facilitates real-time monitoring of the affinity  
285 capture process to overcome the lack of process monitoring in conventional affinity capture  
286 techniques (27). On the other hand, knowing the N-glycan structures on  $\beta_2$ -Tf allows for the  
287 design of other novel test methods for  $\beta_2$ -Tf in the future. For instance, it is possible to employ  
288 carbohydrate-binding reagents to selectively capture  $\beta_2$ -Tf for MS analysis or to establish  
289 antibody-lectin Sandwich immunoassays.

290

## 291 **Acknowledgment**

292

293 The authors thank Gator Bio (Palo Alto, CA) and CMP Scientific (Brooklyn, NY) for kindly  
294 providing equipment and consumables, and C. Wong, S. Ferolino, L. Calayag, and R. Rieta at  
295 Stanford Health Care for collecting samples for this research.

296

## 297 **References**

298

- 299 1. Warnecke A, Averbek T, Wurster U, Harmening M, Lenarz T, Stöver T. Diagnostic  
300 Relevance of  $\beta$ 2-Transferrin for the Detection of Cerebrospinal Fluid Fistulas. Arch  
301 Otolaryngol Neck Surg. 2004 Oct 1;130(10):1178.
- 302 2. McCudden CR, Senior BA, Hainsworth S, Oliveira W, Silverman LM, Bruns DE, et al.  
303 Evaluation of high resolution gel  $\beta$  2 -transferrin for detection of cerebrospinal fluid leak.  
304 Clin Chem Lab Med CCLM. 2013 Feb 1;51(2):311–5.
- 305 3. Papadea C, Schlosser RJ. Rapid Method for  $\beta$ 2-Transferrin in Cerebrospinal Fluid Leakage  
306 Using an Automated Immunofixation Electrophoresis System. Clin Chem. 2005 Feb  
307 1;51(2):464–70.
- 308 4. Görögh T, Rudolph P, Meyer JE, Werner JA, Lippert BM, Maune S. Separation of  $\beta$ 2-  
309 Transferrin by Denaturing Gel Electrophoresis to Detect Cerebrospinal Fluid in Ear and  
310 Nasal Fluids. Clin Chem. 2005 Sep 1;51(9):1704–10.
- 311 5. Zaret DL, Morrison N, Gulbranson R, Keren DF. Immunofixation to Quantify  $\beta$ 2-Transferrin  
312 in Cerebrospinal Fluid to Detect Leakage of Cerebrospinal Fluid from Skull Injury. Clin  
313 Chem. 1992 Sep 1;38(9):1909–12.
- 314 6. Nandapalan V, Watson ID, Swift AC. Beta-2-transferrin and cerebrospinal fluid rhinorrhoea.  
315 Clin Otolaryngol. 1996 Jun;21(3):259–64.
- 316 7. Gallo P, Bracco F, Morara S, Battistin L, Tavolato B. The cerebrospinal fluid transferrin/Tau  
317 proteins. J Neurol Sci. 1985 Aug;70(1):81–92.
- 318 8. Yang F, Lum JB, McGill JR, Moore CM, Naylor SL, van Bragt PH, et al. Human transferrin:  
319 cDNA characterization and chromosomal localization. Proc Natl Acad Sci. 1984  
320 May;81(9):2752–6.
- 321 9. MacGillivray RT, Mendez E, Sinha SK, Sutton MR, Lineback-Zins J, Brew K. The complete  
322 amino acid sequence of human serum transferrin. Proc Natl Acad Sci. 1982 Apr;79(8):2504–  
323 8.
- 324 10. Wang S, Kaltashov IA. Identification of Reduction-Susceptible Disulfide Bonds in  
325 Transferrin by Differential Alkylation Using O <sup>16</sup> /O <sup>18</sup> Labeled Iodoacetic Acid. J Am Soc  
326 Mass Spectrom. 2015 May 1;26(5):800–7.
- 327 11. de Jong G, van Dijk JP, van Eijk HG. The biology of transferrin. Clin Chim Acta. 1990  
328 Sep;190(1–2):1–46.
- 329 12. de Jong G, van Eijk HG. Microheterogeneity of human serum transferrin: A biological  
330 phenomenon studied by isoelectric focusing in immobilized pH gradients. Electrophoresis.  
331 1988;9(9):589–98.
- 332 13. de Jong G, van Noort WL, van Eijk HG. Carbohydrate analysis of transferrin subfractions  
333 isolated by preparative isoelectric focusing in immobilized pH gradients. Electrophoresis.  
334 1992;13(1):225–8.

- 335 14. Delaroche O, Bordureb P, Lippert E, Sagnieza M. Perilymph detection by  $\beta$ 2-transferrin  
336 immunoblotting assay. Application to the diagnosis of perilymphatic fistulae. *Clin Chim*  
337 *Acta*. 1996 Feb;245(1):93–104.
- 338 15. Hoffmann A, Nimtz M, Getzlaff R, Conradt HS. ‘Brain-type’ *N*-glycosylation of asialo-  
339 transferrin from human cerebrospinal fluid. *FEBS Lett*. 1995 Feb 13;359(2–3):164–8.
- 340 16. Futakawa S, Nara K, Miyajima M, Kuno A, Ito H, Kaji H, et al. A unique N-glycan on  
341 human transferrin in CSF: a possible biomarker for iNPH. *Neurobiol Aging*. 2012  
342 Aug;33(8):1807–15.
- 343 17. Brown KJ, Vanderver A, Hoffman EP, Schiffmann R, Hathout Y. Characterization of  
344 transferrin glycopeptide structures in human cerebrospinal fluid. *Int J Mass Spectrom*. 2012  
345 Feb;312:97–106.
- 346 18. Nagae M, Morita-Matsumoto K, Arai S, Wada I, Matsumoto Y, Saito K, et al. Structural  
347 change of N-glycan exposes hydrophobic surface of human transferrin. *Glycobiology*. 2014  
348 Aug 28;24(8):693–702.
- 349 19. Hoshi K, Ito H, Abe E, Fuwa TJ, Kanno M, Murakami Y, et al. Transferrin Biosynthesized  
350 in the Brain Is a Novel Biomarker for Alzheimer’s Disease. *Metabolites*. 2021 Sep  
351 10;11(9):616.
- 352 20. Hoshi K, Matsumoto Y, Ito H, Saito K, Honda T, Yamaguchi Y, et al. A unique glycan-  
353 isoform of transferrin in cerebrospinal fluid: A potential diagnostic marker for neurological  
354 diseases. *Biochim Biophys Acta BBA - Gen Subj*. 2017 Oct;1861(10):2473–8.
- 355 21. Caslavaska J, Schild C, Thormann W. High-resolution capillary zone electrophoresis and  
356 mass spectrometry for distinction of undersialylated and hypoglycosylated transferrin  
357 glycoforms in body fluids. *J Sep Sci*. 2020 Jan;43(1):241–57.
- 358 22. Siuti N, Kelleher NL. Decoding protein modifications using top-down mass spectrometry.  
359 *Nat Methods*. 2007 Oct;4(10):817–21.
- 360 23. Brown KA, Melby JA, Roberts DS, Ge Y. Top-down proteomics: challenges, innovations,  
361 and applications in basic and clinical research. *Expert Rev Proteomics*. 2020 Oct  
362 2;17(10):719–33.
- 363 24. Luo RY, Wong C, Xia JQ, Glader BE, Shi RZ, Zehnder JL. Neutral-Coating Capillary  
364 Electrophoresis Coupled with High-Resolution Mass Spectrometry for Top-Down  
365 Identification of Hemoglobin Variants. *Clin Chem*. 2022 Oct 29;hvac171.
- 366 25. Donnelly DP, Rawlins CM, DeHart CJ, Fornelli L, Schachner LF, Lin Z, et al. Best practices  
367 and benchmarks for intact protein analysis for top-down mass spectrometry. *Nat Methods*.  
368 2019 Jul;16(7):587–94.



- 369 26. Padula M, Berry I, O'Rourke M, Raymond B, Santos J, Djordjevic SP. A Comprehensive  
370 Guide for Performing Sample Preparation and Top-Down Protein Analysis. *Proteomes*. 2017  
371 Apr 7;5(4):11.
- 372 27. Luo RY, Yang S. Using Microprobe-Capture In-Emitter Elution to Directly Couple Label-  
373 Free Optical Sensing Technology with Mass Spectrometry for Top-Down Protein Analysis  
374 [Internet]. *Chemistry*; 2022 Oct [cited 2022 Oct 25]. Available from:  
375 <https://chemrxiv.org/engage/chemrxiv/article-details/6352339055a0816c28bee4cb>
- 376 28. Luo YR, Chakraborty I, Lazar-Molnar E, Wu AHB, Lynch KL. Development of Label-Free  
377 Immunoassays as Novel Solutions for the Measurement of Monoclonal Antibody Drugs and  
378 Antidrug Antibodies. *Clin Chem*. 2020 Oct 1;66(10):1319–28.
- 379 29. Luo YR, Yun C, Chakraborty I, Wu AHB, Lynch KL. A SARS-CoV-2 Label-Free Surrogate  
380 Virus Neutralization Test and a Longitudinal Study of Antibody Characteristics in COVID-  
381 19 Patients. Tang YW, editor. *J Clin Microbiol* [Internet]. 2021 Jun 18 [cited 2021 Nov  
382 4];59(7). Available from: <https://journals.asm.org/doi/10.1128/JCM.00193-21>
- 383 30. Bieberich E. Synthesis, Processing, and Function of N-glycans in N-glycoproteins. In: Yu  
384 RK, Schengrund CL, editors. *Glycobiology of the Nervous System* [Internet]. New York,  
385 NY: Springer New York; 2014 [cited 2021 Dec 6]. p. 47–70. (*Advances in Neurobiology*;  
386 vol. 9). Available from: [http://link.springer.com/10.1007/978-1-4939-1154-7\\_3](http://link.springer.com/10.1007/978-1-4939-1154-7_3)
- 387 31. Cao L, Diedrich JK, Ma Y, Wang N, Pauthner M, Park SKR, et al. Global site-specific  
388 analysis of glycoprotein N-glycan processing. *Nat Protoc*. 2018 Jun;13(6):1196–212.
- 389 32. Maier M, Reusch D, Bruggink C, Bulau P, Wuhrer M, Mølhøj M. Applying mini-bore  
390 HPAEC-MS/MS for the characterization and quantification of Fc N-glycans from  
391 heterogeneously glycosylated IgGs. *J Chromatogr B*. 2016 Oct;1033–1034:342–52.
- 392 33. Kleinert P, Kuster T, Durka S, Ballhausen D, Bosshard NU, Steinmann B, et al. Mass  
393 Spectrometric Analysis of Human Transferrin in Different Body Fluids. *Clin Chem Lab  
394 Med*. 2003 Jan 4;41(12):1580–8.
- 395 34. Coddeville B, Carchon H, Jaeken J, Briand G, Spik G. Determination of glycan structures  
396 and molecular masses of the glycovariants of serum transferrin from a patient with  
397 carbohydrate deficient syndrome type II. *Glycoconj J*. 1998;15(3):265–73.
- 398 35. HYDRAGEL 6  $\beta$ 2 TRANSFERRIN(E) Kit Instruction Manual. Sebia; 2011.
- 399 36. Caslavská J, Lanz C, Burda P, Tobler M, Thormann W. Analysis of genetic variants of  
400 transferrin in human serum after desialylation by capillary zone electrophoresis and capillary  
401 isoelectric focusing. *J Sep Sci*. 2017 Jun;40(11):2488–97.
- 402 37. Lee PL, Halloran C, Trevino R, Felitti V, Beutler E. Human transferrin G277S mutation: a  
403 risk factor for iron deficiency anaemia: Transferrin G277S Mutation and Anaemia. *Br J  
404 Haematol*. 2001 Nov;115(2):329–33.

- 405 38. Pang H, Koda Y, Soejima M, Kimura H. Identification of a mutation (A1879G) of transferrin  
406 from cDNA prepared from peripheral blood cells. *Ann Hum Genet.* 1998 May;62(3):271–4.
- 407 39. Evans RW, Crawley JB, Garratt RC, Grossmann JG, Neu M, Aitken A, et al.  
408 Characterization and Structural Analysis of a Functional Human Serum Transferrin Variant  
409 and Implications for Receptor Recognition. *Biochemistry.* 1994 Oct 18;33(41):12512–20.

410

411 **Tables**

412

413 Table 1. The MPIE-ESI-MS results of 12 secretion samples from patients suspected of CSF leak.

| Secretion Sample  | $\beta$ 1-Tf |                         | $\beta$ 2-Tf |                         |
|-------------------|--------------|-------------------------|--------------|-------------------------|
|                   | Detected?    | Measured Molecular Mass | Detected?    | Measured Molecular Mass |
| Positive Sample 1 | Yes          | 79554.50 Da             | Yes          | 78008.42 Da             |
| Positive Sample 2 | Yes          | 79554.79 Da             | Yes          | 78008.60 Da             |
| Positive Sample 3 | Yes          | 79554.75 Da             | Yes          | 78008.83 Da             |
| Positive Sample 4 | Yes          | 79554.04 Da             | Yes          | 78008.68 Da             |
| Positive Sample 5 | Yes          | 79554.77 Da             | Yes          | 78008.03 Da             |
| Negative Sample 1 | Yes          | 79554.29 Da             | No           | /                       |
| Negative Sample 2 | Yes          | 79554.80 Da             | No           | /                       |
| Negative Sample 3 | Yes          | 79554.81 Da             | No           | /                       |
| Negative Sample 4 | No           | /                       | No           | /                       |
| Negative Sample 5 | No           | /                       | No           | /                       |
| Negative Sample 6 | Yes          | 79554.49 Da             | No           | /                       |
| Negative Sample 7 | Yes          | 79554.73 Da             | No           | /                       |

414

415 **Figure Captions**

416

417 Figure 1. (A) Experiment workflow of MPIE-ESI-MS for Tf analysis. The MPIE-ESI-MS results  
418 of (B) a serum sample, (C) a CSF sample, and (D) a secretion sample from a patient diagnosed of  
419 CSF leak: HR-MS raw mass spectra (left) and deconvoluted mass spectra (right) of captured Tf  
420 molecules, showing serum-type Tf in (B), and both serum-type Tf and brain-type Tf in (C) and  
421 (D).

422

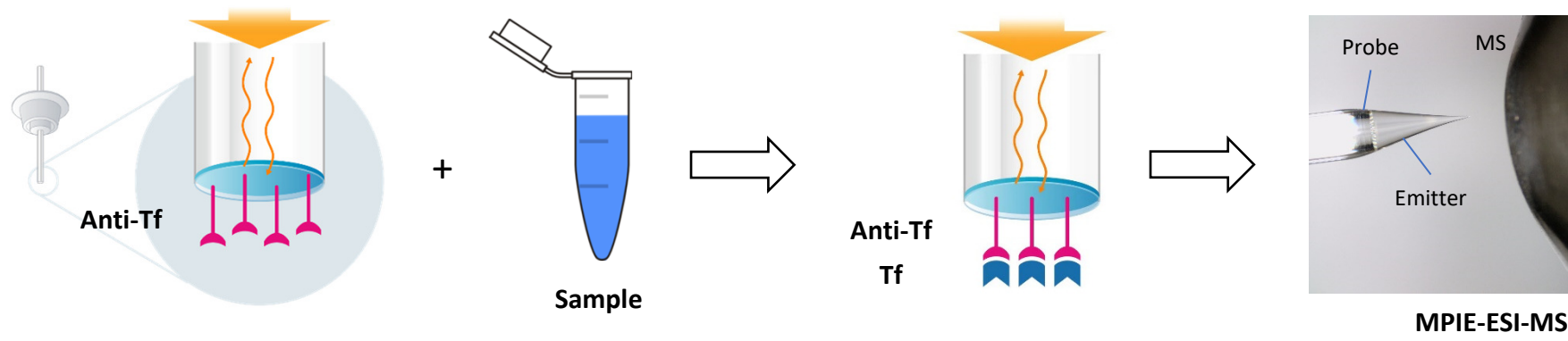
423 Figure 2. The MPIE-ESI-MS results of (A) the extract from the gel stripe of the  $\beta_1$ -Tf band  
424 region and (B) the extract from the gel stripe of the  $\beta_2$ -Tf band region: HR-MS raw mass spectra  
425 (left) and deconvoluted mass spectra (right) of captured Tf molecules, showing  $\beta_1$ -Tf in (B) and  
426  $\beta_2$ -Tf in (C).

427

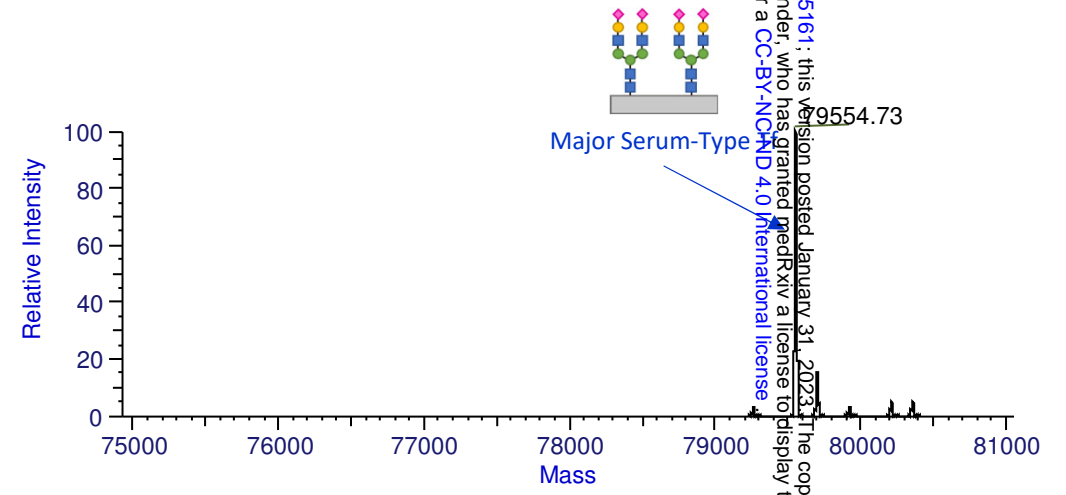
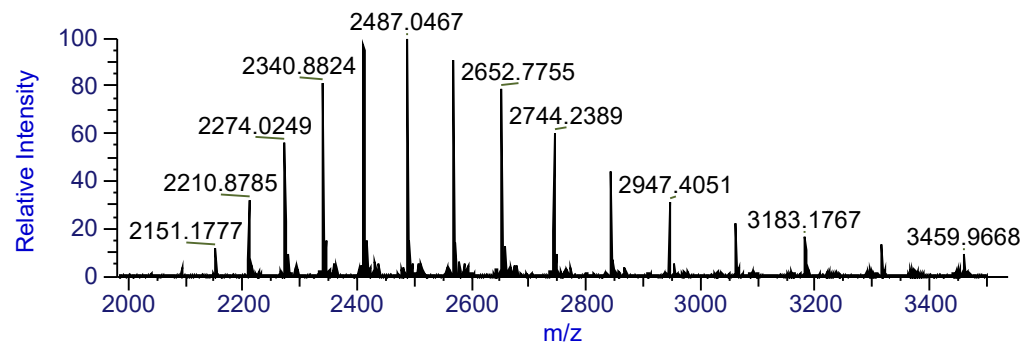
428 Figure 3. (A) Primary structure of human transferrin, showing the sequence of 679 amino acids,  
429 19 disulfide bonds, and 2 N-glycosylation sites. (B) N-glycan structures on  $\beta_1$ -Tf (major serum-  
430 type Tf) and  $\beta_2$ -Tf (major brain-type Tf), confirmed by comparing the theoretical molecular  
431 masses of the Tf glycoforms with the measured molecular masses in Figure 1, Figure 2, and  
432 Table 1.

# Figure 1

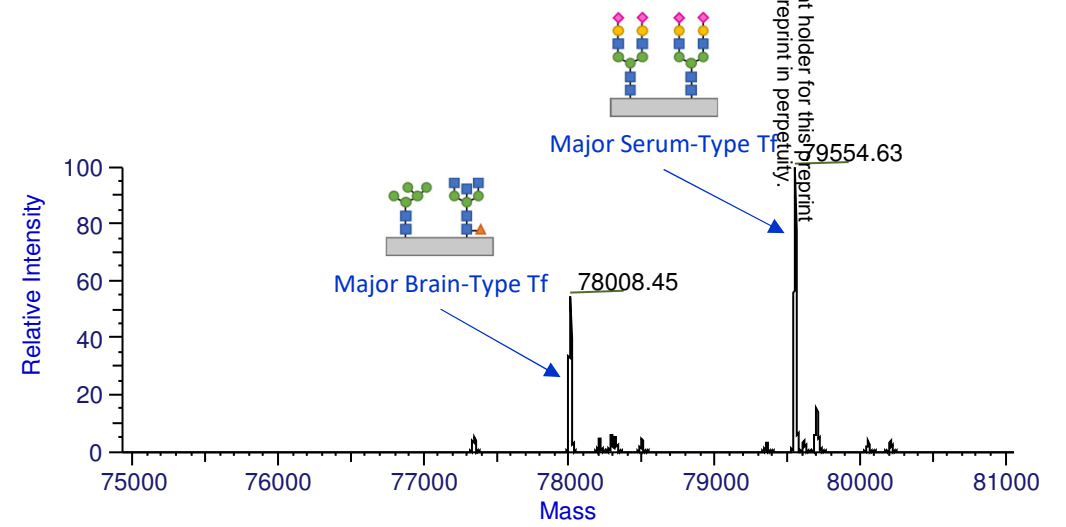
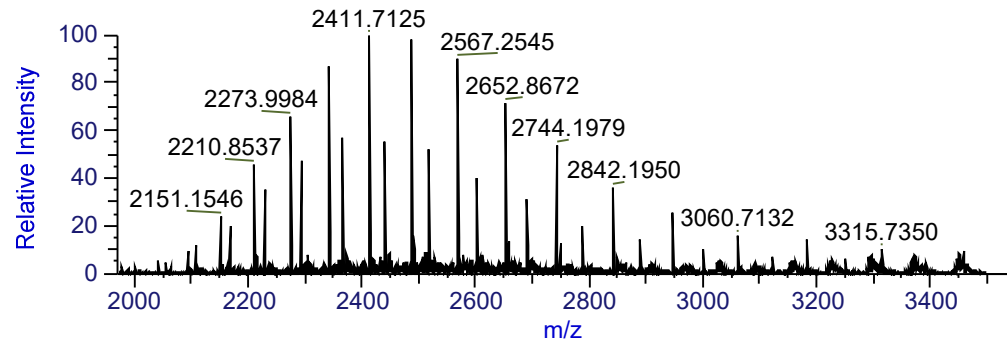
(A)



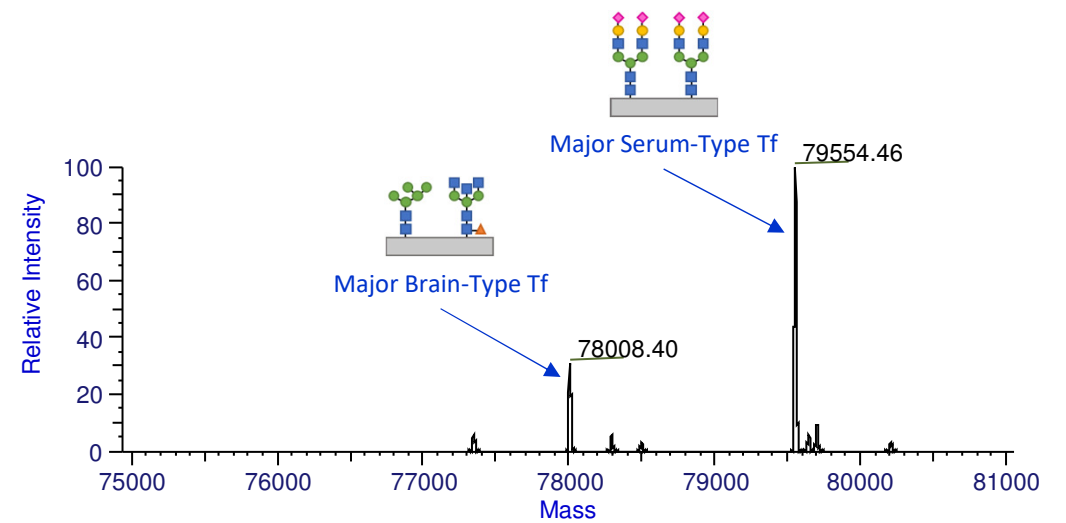
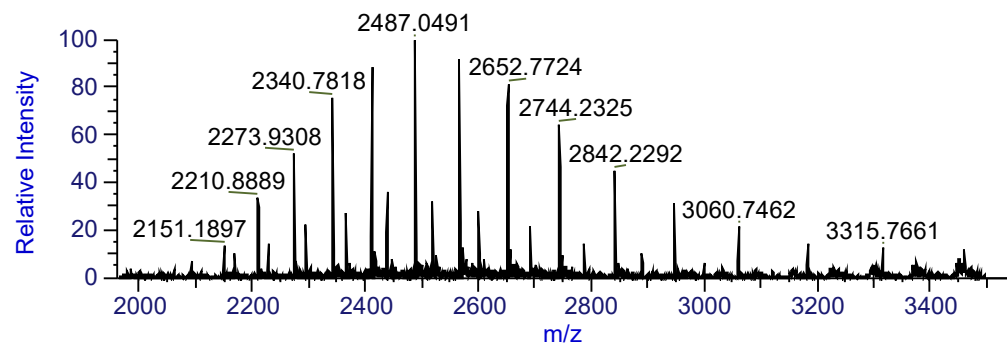
(B)



(C)



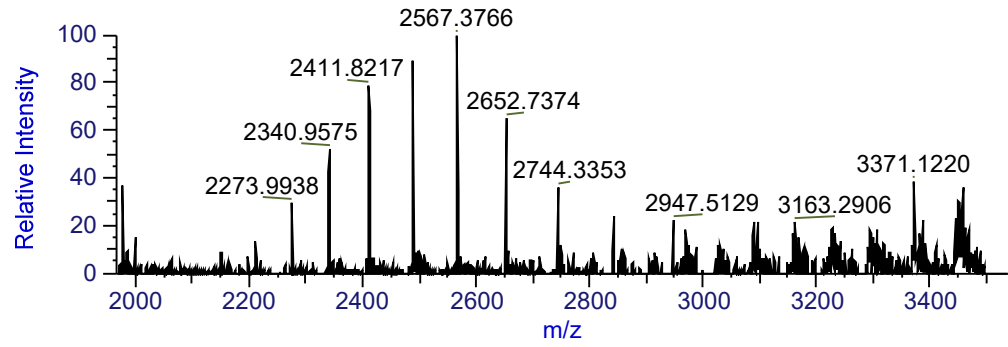
(D)



medRxiv preprint doi: <https://doi.org/10.1101/2023.01.29.23285161>; this version posted January 31, 2023. The copyright holder for this preprint (which was not certified by peer review) is the author/funder, who has granted medRxiv a license to display the preprint in perpetuity. It is made available under a CC-BY-NC-ND 4.0 International license.

# Figure 2

(A)



(B)

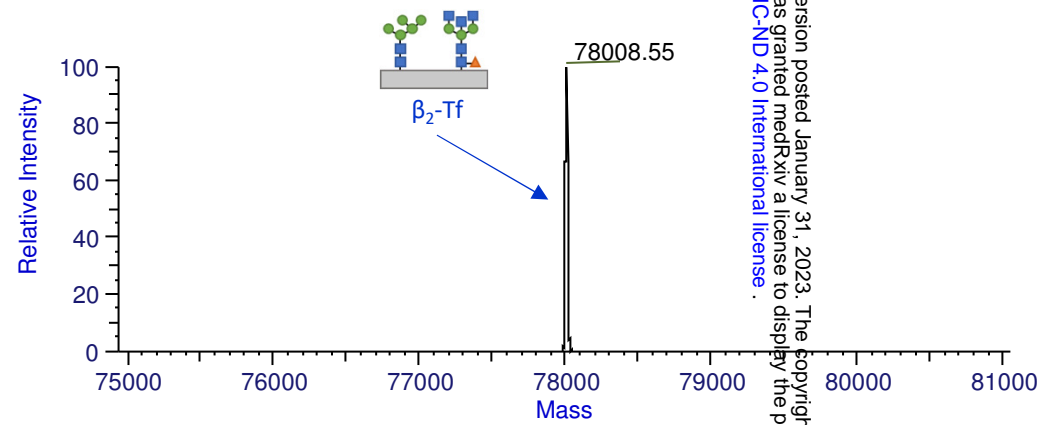
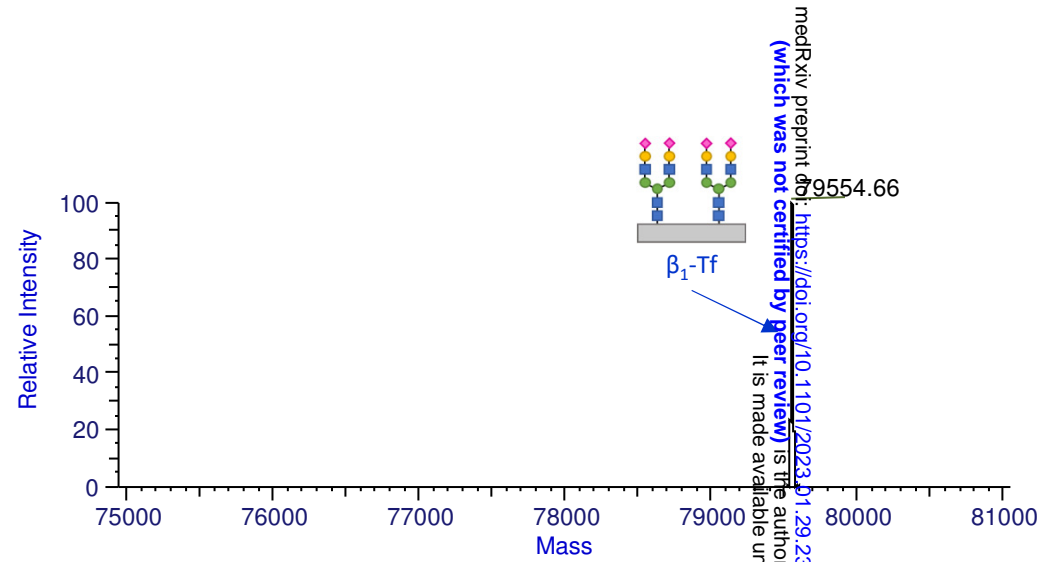
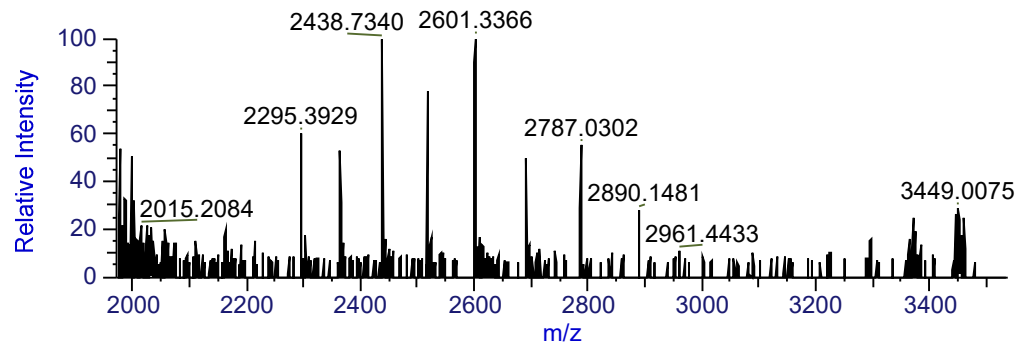
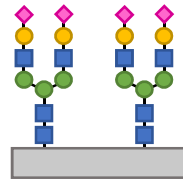


# Figure 3

(A) VPDKTVRWCA VSEHEATKQ SFRDHMKSVI PSDGPSVAQV KKASYLDQIR AIAANEADAV TLDAGLVYDA YLAPNNLKPV VAEFYGSKED  
 PQTFFYAVAV VKKDSGFQMN QLRGKKSCHT GLGRSAGWNI PIGLLYCDLP EPRKPLEKAV ANFFSGSCAP CADGTDFFPQLCQLCPGCCS  
 TLNQYFGYSG AFKCLKDGAG DVAFVKHSTI FENLANKADR DQYELICLDN TRKPVDEYKDCHLAQVPSHT VVARSMGGKE DLIWELLNQA  
 QEHFGKDKSK EFQLFSSPHG KDLLFKDSAH GFLKVPPRMD AKMYLGYEYV TAIRNLREGT CPEAPTDECK PVKWCALSHH ERLKDEWSV  
 NSVGKIEQVS AETTEDCIAK IMNGEADAMS LDGGFVYIAG KQGLVPVLAE NYNKSNDIED TPEAGYFAVA VVKKSASDLT WDNLKGKKS  
 HTAVGRTAGW NIPMGLLYNK INHCRFDEFF SEGCAPGSKK DSSLCKLGMG SGLNLCEPNN KEGYYGYTGA FRCVLVEKGDV AFVKHQTPVQ  
 NTGGKNPDPW AKNLNEKDYE LLCLDGTRKP VEEYANCHLA RAPNHAVVTR KDKEACVHKI LRQQQHLFGS NVTD CSGNFC LFRSETKDLL  
 FRDDTVCLAK LHDRNTYEKY LGEEYVKA VG NLRKQSTSSL LEACTFRRP

Primary Structure of Human Transferrin: 679 AA, 19 Disulfide Bonds (Orange Label), 2 N-Glycosylation Sites (Blue Label)

(B)

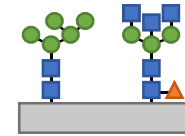


Major Serum-Type Tf  
 Asn413: G2S2  
 Asn611: G2S2

Theoretical Molecular Mass: 79554.71 Da

Measured Molecular Mass: 79554.04 Da – 79554.81 Da

- N-Acetylglucosamine
- Mannose
- Galactose
- ◆ N-Acetylneuraminic Acid
- ▲ Fucose



Major Brain-Type Tf  
 Asn413: M5  
 Asn611: G0FB

Theoretical Molecular Mass: 78008.35 Da

Measured Molecular Mass: 78008.03 Da – 78008.83 Da